Received 27 September 2023; revised 17 November 2023; accepted 7 December 2023. Date of publication 15 December 2023; date of current version 22 January 2024.

Digital Object Identifier 10.1109/OJCOMS.2023.3343665

Energy Efficient Deployment of VLC-Enabled UAV Using Particle Swarm Optimization

HUSSAM IBRAIWISH (Student Member, IEEE), MAHMOUD WAFIK ELTOKHEY (Member, IEEE), AND MOHAMED-SLIM ALOUINI (Fellow, IEEE)

Division of Computer, Electrical and Mathematical Science and Engineering, King Abdullah University of Science and Technology, Thuwal 23955-6900, Saudi Arabia

CORRESPONDING AUTHOR: H. IBRAIWISH (e-mail: hussam.ibraiwish@kaust.edu.sa)

ABSTRACT Aerial base stations can be realized using unmanned aerial vehicles (UAVs)-mounted access points, which offer flexible and rapid network access in scenarios where terrestrial cellular networks are challenged by high traffic loads or insufficient coverage. Visible light communication (VLC) is an emerging technology that can be integrated with UAVs to offer simultaneous communication and illumination services while having low interference, high energy efficiency, and high data rates. To achieve an efficient operation of VLC-enabled UAVs, the power consumption of the UAVs due to their mobility should be considered, as it constitutes a significant portion of the total power consumption of the UAVs, especially when compared to that of the communication needs. This paper proposes a framework to optimize the trajectories of VLC-enabled UAVs, considering a multi-objective optimization problem that jointly maximizes the sum-rate and rate fairness of the users and minimizes the power consumption of the UAVs using particle swarm optimization (PSO) algorithm. The results show that the proposed optimization can effectively improve the performance of the system under various user mobility scenarios and UAV deployment altitudes.

INDEX TERMS Visible light communication (VLC), unmanned aerial vehicles (UAVs), multi-objective optimization, particle swarm optimization (PSO), trajectory optimization.

I. INTRODUCTION

THE SIXTH generation (6G) of wireless networks is expected to provide unprecedented levels of data rate, latency, reliability, and connectivity for various applications [1]. However, the rapid increase in the number of connected devices and the diversity of the network service requirements may pose cost and performance challenges for the existing terrestrial networks [2]. A promising solution for these challenges is to deploy aerial base stations, also known as unmanned aerial vehicles (UAVs)-mounted base stations, which can flexibly support congested networks and provide coverage in rural areas where building permanent base stations is not economical [3]. Nevertheless, using radio frequency (RF)-based transmissions with the UAVs may introduce interference with terrestrial networks, adversely affecting the performance of both aerial and terrestrial networks [4]. Furthermore, as the public concern about the health and environmental impacts of electromagnetic field (EMF) exposure rises, more stringent regulations on RF technologies are being imposed, which may further constrain the data rates supported by the UAVs [5]. These factors motivate exploring alternative electromagnetic spectrum bands with the UAVs, which can offer more spectrum availability, higher data rates, lower interference, and lower EMF exposure.

Visible light communication (VLC) is an emerging technology that can be integrated with UAVs to enable simultaneous communication and lighting services, which can potentially deliver a promising solution for various applications, such as search and rescue operations. VLC-enabled UAVs can achieve high energy efficiency since light-emitting diodes (LEDs) are employed as both data transmitters and luminaires, which reduces the need for additional hardware and energy consumption [6]. Moreover, they can provide advantages such as wide license-free

bandwidth, low cost, high data rates, and low interference. However, VLC-enabled UAVs also face several challenges that need to be addressed for their effective deployment and operation. One of the main challenges is the limitations on coverage area [7], which results from the high dependence on factors such as line-of-sight (LOS) conditions, the angle of incidence, and the angle of irradiance. Another challenge is the inter-cell interference [8], which can degrade the performance of the VLC networks due to a lack of control over the directivity of VLC transmitters. Therefore, it is essential to design an efficient and robust deployment scheme for VLC-enabled UAVs to mitigate these difficulties and ensure reliable communication and lighting performance.

The deployment of VLC-enabled UAV systems has been attracting considerable attention recently, especially for improving the network performance and increasing the energy efficiency of the system [4], [9], [10], [11], [12], [13], [14], [15], [16], [17]. Particularly, in [9] and [10], the UAV location in single-UAV networks was optimized to maximize the network sum-rate. Also, in the case of multi-UAV networks, the work in [11] optimized the UAVs locations to simultaneously improve the network sum-rate and reduce the condition number of the channel matrix. As for improving the energy efficiency of the system, the authors of [12] jointly optimized the location, user association, and power allocation of multiple UAVs to minimize the transmit power of the UAVs. The work in [4] took into account the interference caused by ambient illumination, which was predicted using deep learning, while inter-UAV interference was considered in [14]. Also, to further reduce the transmit power of the UAVs, reconfigurable intelligent surfaces (RISs) were employed in [13], and the number of employed UAVs was considered as an additional optimization variable in [15]. The authors of [16] used multi-agent reinforcement learning to jointly maximize the network sum-rate and minimize the UAVs transmit power, whereas the authors of [17] considered a different objective, which sought to increase the coverage probability and decrease the data rate disparity among the users in single-UAV networks.

Although optimizing the UAVs locations could improve the network performance and reduce the UAV transmission power, deploying rotary-wing UAVs at fixed locations does not necessarily minimize the overall power consumption since they tend to have the lowest power consumption at a non-zero velocity [18]. As a result, not accounting for the power consumption of the UAVs when optimizing their locations could lead to a degradation in the overall energy efficiency, especially when adapting to user mobility. Moreover, the flight power consumption of the UAVs is much higher than their communication power consumption [18], which makes it a crucial factor when deploying the UAVs, especially considering their limited battery capacity and the scarcity of recharging stations in some scenarios. For example, in disaster relief scenarios, where VLC-enabled UAVs can provide both wireless coverage and illumination for rescue teams and survivors, the terrestrial infrastructure may be compromised or unreachable. Hence, it is essential to account for the power consumption of the UAVs to prolong their mission time and ensure a reliable operation. In this paper, we propose optimizing the trajectories of VLC-enabled UAVs to maximize the network sum-rate and rate fairness while minimizing the power consumption in multi-UAV networks. To the best of our knowledge, none of the previous works considered the mobility power consumption of the UAVs, which could be significant if not taken into account. To tackle this problem, we use particle swarm optimization (PSO), a bio-inspired optimization approach that mimics the collective behavior of swarms, which has been shown to be effective in solving various VLC-related problems in the literature [19], [20]. The main contribution of this work is summarized as follows:

- We develop a framework for optimizing the trajectories of VLC-enabled UAVs that jointly maximizes the sum-rate and rate fairness, and minimizes the power consumption in multi-UAV networks.
- We tackle this problem by applying PSO and conducting a systematic analysis of the PSO parameters to determine the configuration that ensures a balanced trade-off between exploration and exploitation. Moreover, we investigate the impact of incorporating the previous locations of the UAVs in the initialization step.
- We conduct a comprehensive analysis of how the UAVs altitude influences the system performance under the proposed optimization scheme, taking into account various user mobility scenarios. Furthermore, we conduct a trade-off analysis of the proposed optimization, which allows us to adapt the proposed algorithm for various preferences profiles.

The rest of the paper is structured as follows. Section II introduces the system model and the main assumptions. Section III presents the considered optimization problem. Section IV describes the proposed optimization algorithm. Section V presents the simulation results, including the parameter selection, the convergence analysis, the effect of UAVs altitude on the performance of the system, the interference management methods, and the trade-off analysis between the considered objectives. Finally, conclusions are drawn in Section VI.

II. SYSTEM MODEL

We consider a system of N UAVs supporting lighting and communication for K users, as shown in Fig. 1. At time t, the k^{th} user and n^{th} UAV are located at $(s_k(t), w_k(t), 0)$ and $(x_n(t), y_n(t), H)$, respectively. Here, intensity modulation and direct detection (IM/DD) is employed, where the UAVs are equipped with LED luminaires that emit optical intensities proportional to the signal amplitudes. Ground users, on the other hand, are equipped with photodetectors, which capture the transmitted optical intensities and demodulate them to retrieve the signal amplitudes.

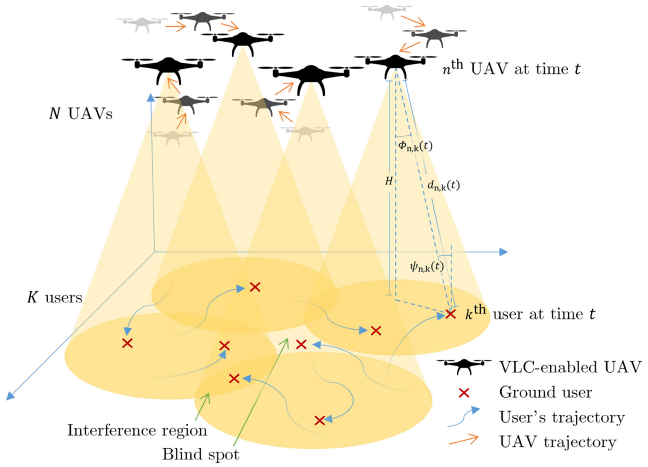

FIGURE 1. An illustration of the system model with N UAVs and K mobile users.

A. CHANNEL MODEL

Operating at relatively high altitudes enables the UAVs to establish LOS communication links with ground users with a high probability. Moreover, this results in the dominance of the LOS signal strength over the non-LOS (NLOS) signals, which improves the quality of service of the network. Assuming a Lambertian radiation pattern and neglecting the NLOS signals, the channel gain between the n^{th} UAV and the k^{th} user at time t is calculated as [21]:

$$h_{n,k}(t) = \frac{(m+1)A\,\eta}{2\pi\, d_{n,k}^2(t)} g\big(\psi_{n,k}(t)\big)\cos^m\big(\phi_{n,k}(t)\big)\cos\big(\psi_{n,k}(t)\big), \tag{1}$$

where

$$g\big(\psi_{n,k}(t)\big) = \begin{cases} \frac{r_e^2}{\sin^2(\Psi_c)}, & 0 \le \psi_{n,k}(t) \le \Psi_c \\ 0, & \psi_{n,k}(t) > \Psi_c \end{cases}, \tag{2}$$

where $d_{n,k}(t)$, $\phi_{n,k}(t)$, and $\psi_{n,k}(t)$ are the link distance, angle of irradiance, and angle of incidence between the n^{th} UAV and the k^{th} user, respectively, as shown in Fig. 1, m is the Lambertian order of the transmitted optical beam, A is the area of the photodetector, η is the responsivity of the photodetector, $g(\psi_{n,k}(t))$ is the gain of the optical concentrator deployed at the receiver, r_e is the refractive index of the concentrator, and Ψ_c is the field of view (FOV) semi-angle of the receiver.

We consider a system where all the UAVs share the same channel and adopt an orthogonal resource allocation scheme, such as time division multiplexing, to allocate resources among ground users. This implies that some users at the cell edge may experience inter-UAV interference due to the simultaneous reception of multiple signals. To account for this, we consider the signal-to-noise-plus-interference ratio (SINR) as the performance metric for the communication quality of each user. The SINR for the k^{th} user can be computed as:

$$\text{SINR}_k(t) = \frac{\left(\sum_{n=1}^{N} u_{n,k}(t)\, h_{n,k}(t)\, P\right)^2}{N_0\, BW + \sum_{n=1}^{N}\left(\big(1-u_{n,k}(t)\big)\, h_{n,k}(t)\, P\right)^2}, \tag{3}$$

where $u_{n,k}(t)$ is a binary variable that indicates the association of the k^{th} user with the n^{th} UAV, P is the transmitted power, N_0 is the noise power spectral density, and BW is the system bandwidth. Employing IM/DD imposes a non-negativity constraint on the input signal, where a tight lower bound of the capacity of VLC systems under both the non-negativity and average optical power constraints is derived in [22]. Under the assumption that the considered channel coding scheme achieves this lower bound, the data rate of the k^{th} user at time t equals:

$$r_k(t) = \frac{BW}{2\, G_k(t)} \log_2\Big(1 + \frac{e}{2\pi}\,\text{SINR}_k(t)\Big), \tag{4}$$

where $G_k(t)$ is the number of users who share the same UAV association with the k^{th} user. Assuming that each user is served by the UAV that provides the highest channel gain, $u_{n,k}(t)$ is calculated as:

$$u_{n,k}(t) = \begin{cases} 1, & n = \underset{i}{\text{argmax}}\, h_{i,k}(t) \\ 0, & \text{otherwise} \end{cases}. \tag{5}$$

Deploying the UAVs to maximize the network sum-rate is a potential way to improve the system performance. However, this may lead to an unfair solution, as some users may be prioritized over others. Therefore, we also incorporate rate fairness as another objective in our optimization problem, represented by Jain's fairness index, which is defined as [23]:

$$\mathcal{J}(\boldsymbol{r}(t)) = \frac{1}{K}\frac{\left(\sum_{k=1}^{K} r_k(t)\right)^2}{\sum_{k=1}^{K} r_k(t)^2}, \tag{6}$$

where $\boldsymbol{r}(t) = [r_1(t), r_2(t), \ldots, r_K(t)]$.

B. UAV POWER CONSUMPTION MODEL

The mobility of the users may require the UAVs to adjust their positions dynamically to maintain a reliable communication link. However, this may incur high power consumption for the UAVs, which should be considered when optimizing their trajectories. To compute the power consumption of the UAVs, we follow the approach of [24] and [25], which divides the trajectory of the UAV into segments and assumes a constant velocity within each segment. Then, the power consumption is computed based on the model derived in [18] for a rotary-wing UAV traveling along a straight line. Specifically, for the n^{th} UAV traveling with a velocity of v_n, the power consumption is given by:

$$q_n = \underbrace{P_0\left(1 + \frac{3v_n^2}{U_{\text{tip}}^2}\right)}_{\text{blade profile}} + \underbrace{P_1\left(\sqrt{1 + \frac{v_n^4}{4v_0^4}} - \frac{v_n^2}{2v_0^2}\right)^{1/2}}_{\text{induced}} + \underbrace{\frac{1}{2} d_0 \rho s A_r v_n^3}_{\text{parasite}}, \tag{7}$$

where P_0 and P_1 represent the blade power and induced power in hovering status, respectively. U_{tip} denotes the tip

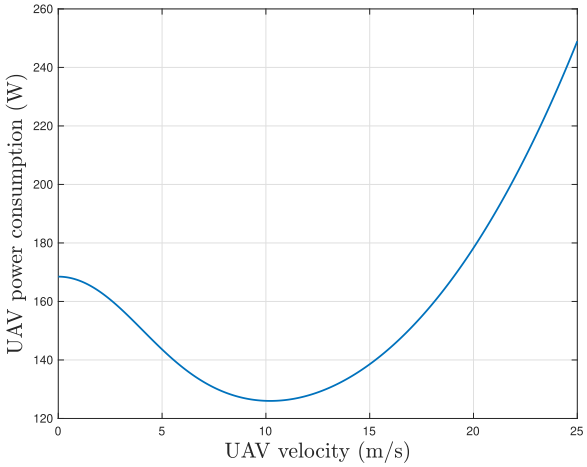

FIGURE 2. The relationship between the power consumption of a rotary-wing UAV and its velocity [18].

speed of the rotor blade, v_0 is the mean rotor induced velocity in hover, d_0 is the fuselage drag ratio, s is the rotor solidity, ρ is the air density, and A_r is rotor disc area. Figure 2 depicts the UAV propulsion power consumption as a function of its velocity using the parameters in [18]. It should be noted that static deployment of the UAVs does not result in the highest energy efficiency, which highlights the necessity of considering the power consumption of the UAVs when planning their deployment.

III. PROBLEM FORMULATION

In VLC-enabled UAV networks, a high sum-rate and a high rate fairness are desirable objectives. However, when considering mobile users, these objectives may conflict with having a low power consumption of the UAVs. Therefore, an optimization framework that balances the sum-rate, rate fairness, and power consumption is needed. This can be formulated as an optimization problem that seeks to maximize the weighted sum of the average sum-rate and the rate fairness, subtracted by the average power consumption of the UAVs. The general form of this optimization problem is given by:

$$\max_{\boldsymbol{x}(t),\boldsymbol{y}(t)} \ \frac{1}{T}\int_0^T \eta_1 \sum_{k=1}^{K} r_k(t) + \eta_2\, \mathcal{J}(\boldsymbol{r}(t)) - \eta_3 \sum_{n=1}^{N} q_n(t)\, \mathrm{d}t \tag{8a}$$

$$\text{s.t} \ \ r_k(t) \geq R_{\text{th}}, \ \ \forall k \in [1, 2, \ldots, K], \tag{8b}$$

$$\sqrt{(x_n(t) - x_{\tilde{n}}(t))^2 + (y_n(t) - y_{\tilde{n}}(t))^2} \geq d_{\min}, \quad \forall n, \tilde{n} \in [1, 2, \ldots, N], \ n \neq \tilde{n}, \tag{8c}$$

where T is the time interval of interest, during which users move within a square region of length L m. We use the weights η_1, η_2, and η_3 to adjust the contribution of each term to the objective function. The first constraint is to ensure having a minimum data rate of R_{th} for all users. The second constraint is used to prevent collisions between the UAVs by ensuring a minimum separation distance of $d_{\min}$.

The problem above is intractable because the optimization variables are continuous functions with infinite dimensions. Therefore, the problem is approximated to the following discretized version:

$$\max_{\boldsymbol{x},\boldsymbol{y}} \ \frac{\Delta t}{T}\sum_{l=0}^{T/\Delta t}\left(\eta_1 \sum_{k=1}^{K} r_k[l] + \eta_2\, \mathcal{J}(\boldsymbol{r}[l]) - \eta_3 \sum_{n=1}^{N} q_n[l]\right) \tag{9a}$$

$$\text{s.t} \ \ r_k[l] \geq \mathrm{R}_{\text{th}}, \ \ \forall k \in [1, 2, \ldots, K], \tag{9b}$$

$$\sqrt{(x_n[l] - x_{\tilde{n}}[l])^2 + (y_n[l] - y_{\tilde{n}}[l])^2} \leq d_{\min}, \quad \forall n, \tilde{n} \in [1, 2, \ldots, N], \ n \neq \tilde{n}, \tag{9c}$$

where Δt is the considered discretization step and the suffix $[l]$ indicates the variable value at the time instant $l \times \Delta t$. The discrete-time velocity of the n^{th} UAV at the l^{th} time step is obtained by applying the backward difference formula as:

$$v_n[l] = \frac{\sqrt{(x_n[l] - x_n[l-1])^2 + (y_n[l] - y_n[l-1])^2}}{\Delta t}. \tag{10}$$

Even after discretizing the problem, it remains computationally demanding, as it involves a large number of variables. Moreover, it relies on the assumption that the users' movements are predetermined since the UAVs trajectories are optimized in advance, which may not be applicable in some scenarios. Hence, we propose an online approach that dynamically adapts the UAVs locations at each time step based on the current information. The problem is then reformulated as follows:

$$\min_{\boldsymbol{x}[l],\boldsymbol{y}[l]} \ -\eta_1 \sum_{k=1}^{K} r_k[l] - \eta_2\, \mathcal{J}(\boldsymbol{r}[l]) + \eta_3 \sum_{n=1}^{N} q_n[l] + \eta_4\, \overline{N}(R_{\text{th}}) \tag{11a}$$

$$\text{s.t} \ \ L/8 \leq x_1[l], y_1[l], y_2[l], x_3[l] \leq 3L/8, \tag{11b}$$

$$5L/8 \leq x_2[l], y_3[l], x_4[l], y_4[l] \leq 7L/8, \tag{11c}$$

where $\overline{N}(R_{\text{th}})$ is the number of users who are receiving a data rate below R_{th}. The data rate constraint has been handled by adding $\eta_4\, \overline{N}(R_{\text{th}})$ to the objective function, which discards solutions that do not satisfy this constraint, where η_4 is a large coefficient that dominates the other terms when the constraint is violated. As for the UAV separation distance constraint, we relax it by assigning a rectangular area for each UAV, as shown in Fig. 3, where a scenario with four UAVs is considered. This ensures the constraint is met and simplifies the optimization by reducing the search space. However, the relaxed optimization problem is non-convex as it involves multiple non-convex terms. Therefore, the problem may exhibit multiple local maxima, which poses the challenge of avoiding suboptimal solutions with relatively high values.

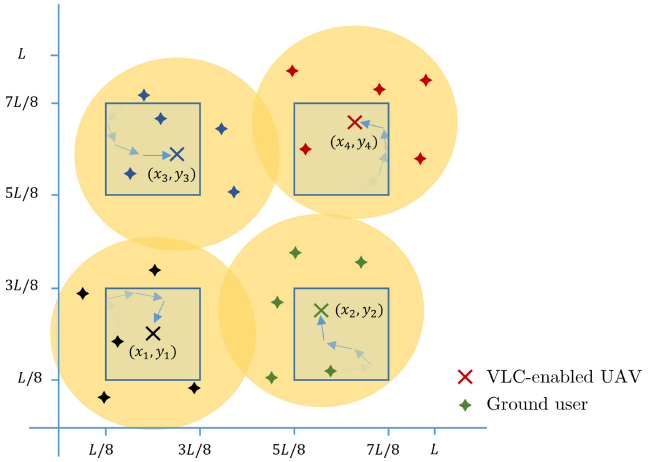

FIGURE 3. The permissible areas for the movements of the four VLC-enabled UAVs that provide illumination and wireless service to twenty users.

IV. PARTICLE SWARM OPTIMIZATION

PSO is a bio-inspired optimization algorithm that mimics the social behavior of a swarm of particles, such as bees, that cooperatively explore the field to find the location with highest density of flowers. In PSO, each particle represents a potential solution to the optimization problem and updates its position in the search space based on its own best position discovered so far (pbest) and the best position discovered by the whole swarm (gbest). After a particle moves to a new position, the objective function is evaluated at that position. If the evaluation result is better than the objective function value at the particle's pbest, then the particle updates its pbest to the new position. Similarly, if the evaluation result is better than the objective function value at the gbest, then the swarm updates its gbest to the new position. The complexity of the PSO algorithm mainly depends on the number of objective function evaluations, which equals the number of iterations multiplied by the number of particles [26].

Let $\boldsymbol{x}_i^{(j)} \in \mathbb{R}^M$ denote the position of the i^{th} particle in the M-dimensional optimization problem at the j^{th} iteration, where J is the total number of iterations. The position update of the particle is given by [27]:

$$\boldsymbol{x}_i^{(j)} = \boldsymbol{x}_i^{(j-1)} + \boldsymbol{v}_i^{(j)}, \tag{12}$$

where $\boldsymbol{v}_i \in \mathbb{R}^M$ is the i^{th} particle's velocity at the j^{th} iteration, which is updated as:

$$\begin{aligned}\boldsymbol{v}_i^{(j)} = w * \boldsymbol{v}_i^{(j-1)} &+ c_1 \,\text{rand}_1(M) * \left(\boldsymbol{p}_{best,i} - \boldsymbol{x}_i^{(j-1)}\right) \\ &+ c_2 \,\text{rand}_2(M) * \left(\boldsymbol{g}_{best} - \boldsymbol{x}_i^{(j-1)}\right),\end{aligned} \tag{13}$$

where $\boldsymbol{p}_{best,i}$ and $\boldsymbol{g}_{best}$ are the i^{th} particle's pbest and the swarm's gbest, respectively. The first term of equation (13) is called the inertia term, which provides a momentum effect that enables the particle to preserve its current velocity to allow it to explore different regions of the search space. The second term is the cognitive term, which attracts the particle toward its own pbest. The third term is the social term, which attracts the particle toward the gbest discovered by the swarm so far. The parameters c_1 and c_2 are often called cognitive and social coefficients, respectively [27]. The cognitive coefficient represents the relative pull of the pbest position; increasing it would encourage the particle to explore the search space. On the other hand, the social coefficient represents the relative pull of the gbest; increasing it would facilitate the convergence to the best solution discovered by the swarm so far. The functions $\text{rand}_1(M)$ and $\text{rand}_2(M)$ return two independent M-dimensional random vectors with uniform distribution ranging from zero to one.

One key factor affecting the convergence of the PSO algorithm is having a balanced trade-off between discovering new areas of the search space, known as exploration and employing the best solutions found so far, known as exploitation [28]. An effective way to enhance exploration in PSO is to increase the swarm size and assign high values to the cognitive coefficient. On the other hand, exploitation can be enhanced by increasing the number of iterations and having a high value of the social coefficient [29]. In general, excessive exploration can result in slow convergence, while excessive exploitation can cause premature convergence to suboptimal solutions [28], [30]. An effective strategy for PSO algorithm is to prioritize exploration in the initial stages and then gradually shift to exploitation in the later stages [31]. In our work, we dynamically adjust the inertia weight, cognitive and social coefficients as [31]:

$$w = 0.9 - 0.5\,\frac{j}{J}, \tag{14}$$

$$c_1 = 2.5 - 2\,\frac{j}{J}, \tag{15}$$

$$c_2 = 0.5 + 2\,\frac{j}{J}. \tag{16}$$

Throughout the algorithm, some particles may exceed the predefined bounds of the problem. We address this by employing the absorbing walls approach [29], which resets the position of the particle to the nearest boundary value and assigns zero velocity to the violated dimension, thus preventing the particles from leaving the search space in the subsequent iteration due to the inertia effect.

V. SIMULATION RESULTS

This section presents the performance evaluation of VLC-enabled UAV networks when solving the proposed optimization problem using PSO. We consider a system with 4 UAVs and 20 users in an area of 80 m × 80 m. The users are mobile and their positions are generated using the random waypoint mobility model [32]. This model assumes that each user moves randomly in an obstacle-free environment. The movement of each user alternates between two phases: travel and pause. During the travel phase, the user randomly selects a destination point within the area of interest and moves towards it in a straight line with a random velocity drawn from a predefined range. During the pause phase, the user remains stationary at the destination

TABLE 1. Simulation parameters.

Parameter	Value
UAV transmit power	15.84 W
Photodetector responsivity	0.4 A/W
Minimum user data rate	0.1 Mbit/s
Lambertian order of the transmitter	1
Photodetector area	10^{-4} m^2
Noise power spectral density	10^{-21} A^2/Hz
Channel bandwidth	10 MHz
Photodetector field-of-view semi-angle	60°
Refractive index of the concentrator	1.5

point for a duration drawn from another predefined range. We consider two mobility scenarios: low mobility and high-mobility, with random velocity values uniformly distributed in [0.1, 1.4] m/s and [0.1, 5.0] m/s, respectively. The random pause time is randomly sampled from 0 to 1 second in both mobility states. The weights η_1, η_2, and η_3 are set to $1/10^8$, 1, and $1/1000$, respectively, which normalizes each term by its order of magnitude and balances their influences on the objective function, while η_4 is set to 100 to ensure the predominance of its corresponding term. Finally, we average the simulation results over 100 independent runs, each lasting for 60 seconds with a discretization step of 0.1 s. Table 1 summarizes the parameters used in the simulations.

A. PARAMETER SELECTION AND ALGORITHM CONVERGENCE

As indicated in the previous section, finding an optimal balance between exploration and exploitation is crucial for the performance of PSO. For a fixed number of objective function evaluations, a trade-off is required between the number of particles and the number of iterations. In this study, we investigate how different combinations of particles and iterations affect the convergence of PSO under low user mobility and a fixed UAVs height of 16 m. We use the excess error as a metric to measure the convergence, which is defined as the difference between the objective function value at the gbest and its value at the final solution obtained by the algorithm. Figure 4 shows the logarithmic scale of the excess error as a function of the evaluation number for different numbers of particles and iterations while keeping the total number of evaluations fixed at 256, where the particles in each iteration are numbered in the order of decreasing excess error. The results indicate that using too few particles and a lot of iterations (e.g., 4 particles and 64 iterations) results in premature convergence to suboptimal solutions due to the lack of exploration of the search space. On the other hand, using a lot of particles and too few iterations (e.g., 32 particles and 8 iterations, or 64 particles and 4 iterations) may facilitate a wider exploration of the search space and result in a better performance in the initial stages. However, the swarm may exhibit slow convergence due to inadequate exploitation of the best positions found by the particles. In our problem, the best results are obtained when the trade-off between the swarm size and the number of iterations is balanced (e.g., using either 8 particles and 32 iterations, or 16 particles and 16 iterations). These settings could minimize the issues of slow convergence and premature convergence that occur when using excessively large or small numbers of particles, respectively.

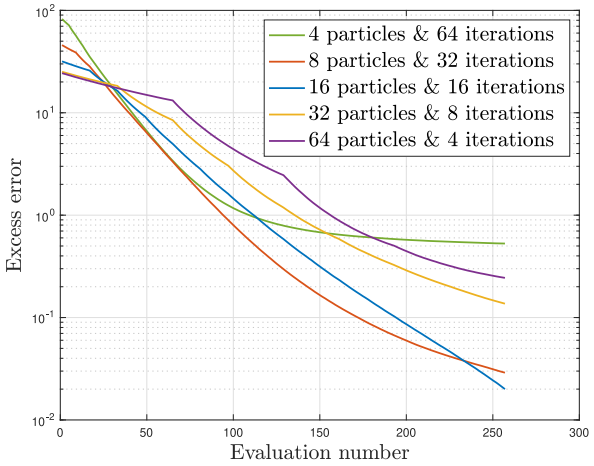

FIGURE 4. Convergence of PSO for different number of particles and iterations.

B. MEMORY-ENHANCED OPTIMIZATION

In the previous simulation, the initial positions and velocities of all particles are randomly assigned following a uniform distribution over the search space, which may lead to slow convergence due to inefficient exploration in the early stages of the optimization process [33]. Indeed, PSO can converge faster by initializing the particles in the regions that are more likely to contain the optimal solution, which would enhance the exploration efficiency of the algorithm. The prior knowledge of such regions is problem-specific and depends on domain knowledge about the problem to be solved. For the considered problem, a promising region to explore in the search space could be in the vicinity of the previous optimal point (assuming that the UAVs were already located there) due to the correlation between the locations of the successive optimal points. The correlation can be analyzed by examining the effect of each term of the objective function as follows:

- The sum-rate, rate fairness, and number of unsatisfied users: maximizing these terms depends on the locations of the users, which do not change significantly over consecutive time steps due to the small time step size. Consequently, the successive optimal locations of the UAVs should be close to each other, which implies a temporal correlation between them. Such correlation is inversely related to the mobility of the users (i.e., low mobility leads to a higher correlation and vice versa). For instance, if the users are stationary, the optimal positions of the UAVs remain unchanged, assuming that they have already converged to the optimal solution. On the other hand, if the users are moving at very high velocities, the successive optimal positions of the UAVs would be highly uncorrelated.

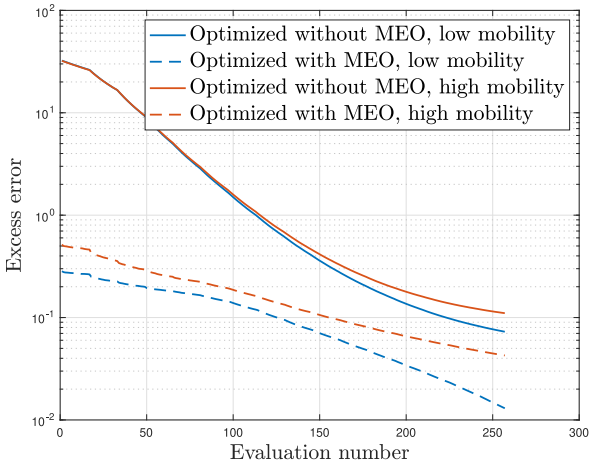

FIGURE 5. Effect of user mobility and considering MEO on the performance of PSO.

- The power consumption of the UAVs: including this term encourages the UAVs to approach the velocity that minimizes their power consumption, which would increase the temporal correlation between the successive optimal locations of the UAVs depending on the considered time step (i.e., according to the considered power consumption model, the optimal velocity is around 10.2 m/s, which corresponds to a distance of 1.02 m for a discretization step of 0.1 s).

To leverage the high temporal correlation of the optimal UAV positions, we propose a memory-enhanced optimization (MEO) scheme, which modifies the particle initialization of PSO to enhance its convergence performance. In MEO, we initialize one particle by setting it to the previous obtained solution, while the rest of the particles are randomly initialized following a uniform distribution within the feasible region. Figure 5 shows the excess error when applying PSO with and without applying MEO for different mobility states. This experiment was conducted with 16 particles and 16 iterations, and the UAVs were set to fly at a height of 16 m. The results reveal that, as expected, MEO accelerates the convergence for both mobility scenarios. In the high mobility scenario, the objective function attains higher values, which can be attributed to the longer travel distances for the UAVs and, consequently, higher power consumption. The low mobility scenario exhibits a larger gap when considering MEO, which demonstrates the advantage of MEO in this case due to the higher correlation of the successive UAV positions.

C. EFFECT OF UAVS ALTITUDE

In this part, we investigate the impact of the UAVs altitude on the system performance, taking into account the proposed optimization scheme. We also examine how considering MEO influences the system under various user mobility scenarios and deployment heights. The altitude of the UAVs is a crucial factor that determines the coverage and interference characteristics of the UAV network, as shown in Figs. 6(a)-6(c), which depict the received SINR distribution in dB across the considered area for three different altitudes of UAVs that are located in the center of their permissible range of movements. As shown in Fig. 6(a), deploying the UAVs at a low altitude results in high SINR values for the users directly below them, owing to the short link distance and the small angle of incidence. However, users at the cell edge encounter large incidence angles that may surpass the receiver's FOV angle, which limits the UAVs coverage and create some regions that are not covered by any UAV, referred to as blind spots. Figure 6(b) shows that increasing the altitude of the UAVs has a trade-off effect on the network performance. On one hand, it reduces the incidence angles for users at cell edges and expands the coverage area of the UAVs. On the other hand, it lowers the SINR for users directly underneath the UAVs and introduces interference for the users at the cell edges. Such interference becomes more severe when increasing UAVs altitude, which leads to a higher degree of overlap among the coverage areas of different UAVs, as shown in Fig. 6

Figures 7(a)-7(d) illustrate the impact of the UAVs altitude on the sum-rate, rate fairness, UAVs power consumption, and number of unsatisfied users, respectively. The figures compare different deployments for the UAVs under low and high user mobility scenarios: non-optimized and optimized UAV locations by PSO with and without MEO, using 16 particles and 16 iterations. In this experiment, low and high altitudes refer to UAVs heights of 10 m and 20 m, respectively. The results show that considering non-optimized UAVs trajectories lead to poor system performance due to blind spot issues at low altitudes, and high interference and low SINR at high altitudes. For instance, as Fig. 7(a) depicts, many users get no coverage when the UAVs are deployed at low altitudes due to the blind spots (e.g., an average of 7 users are out of coverage at a height of 10 m). However, as the UAVs height increases, they provide coverage for more users, and at a height of 16.5 m, full coverage is achieved. However, increasing the UAVs height reduces the overall sum-rate, as the received signal strength deteriorates rapidly with distance due to the path loss, as shown in Fig. 7(c) (e.g., increasing the height from 10 m to 20 m reduces the sum-rate from 97.5 Mbit/s to 60.6 Mbit/s for low user mobility, and from 96.4 Mbit/s to 59.2 Mbit/s for high user mobility). As Fig. 7 illustrates, increasing the UAVs height in the initial stage improves the rate fairness, as the discrepancy between users' data rate reduces due to providing coverage for more users. However, further increasing the UAVs height up to 20 m will deteriorate the rate fairness, as some users may experience the interference issue that adversely impacts their data rates relative to other users (e.g., as the UAVs height increases from 10 m to 13.5 m, the rate fairness improves from 0.462 to 0.675 for low user mobility, and from 0.446 to 0.666 for high user mobility; however, further increasing the UAVs height to 20 m reduces the rate fairness to 0.637 for low user mobility and to 0.627 for high user mobility). When the UAVs

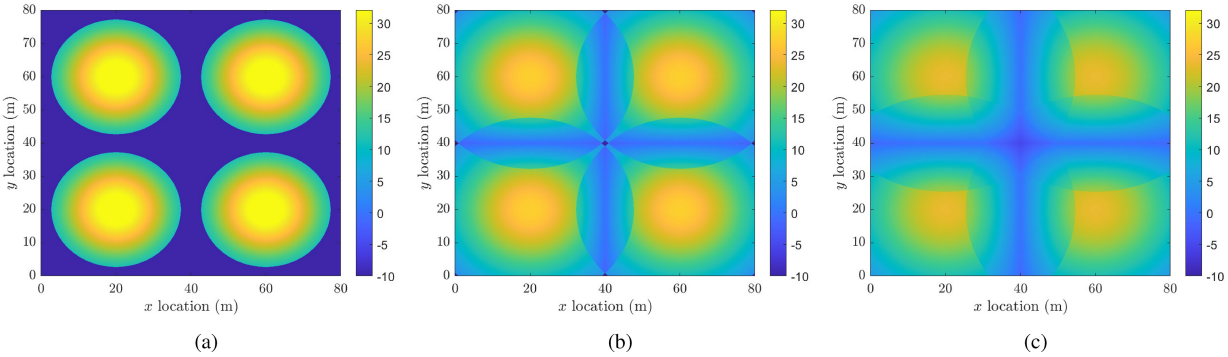

FIGURE 6. Received SINR distribution in dB across the considered area for UAVs altitudes of (a) 10 m, (b) 16 m, and (c) 20 m.

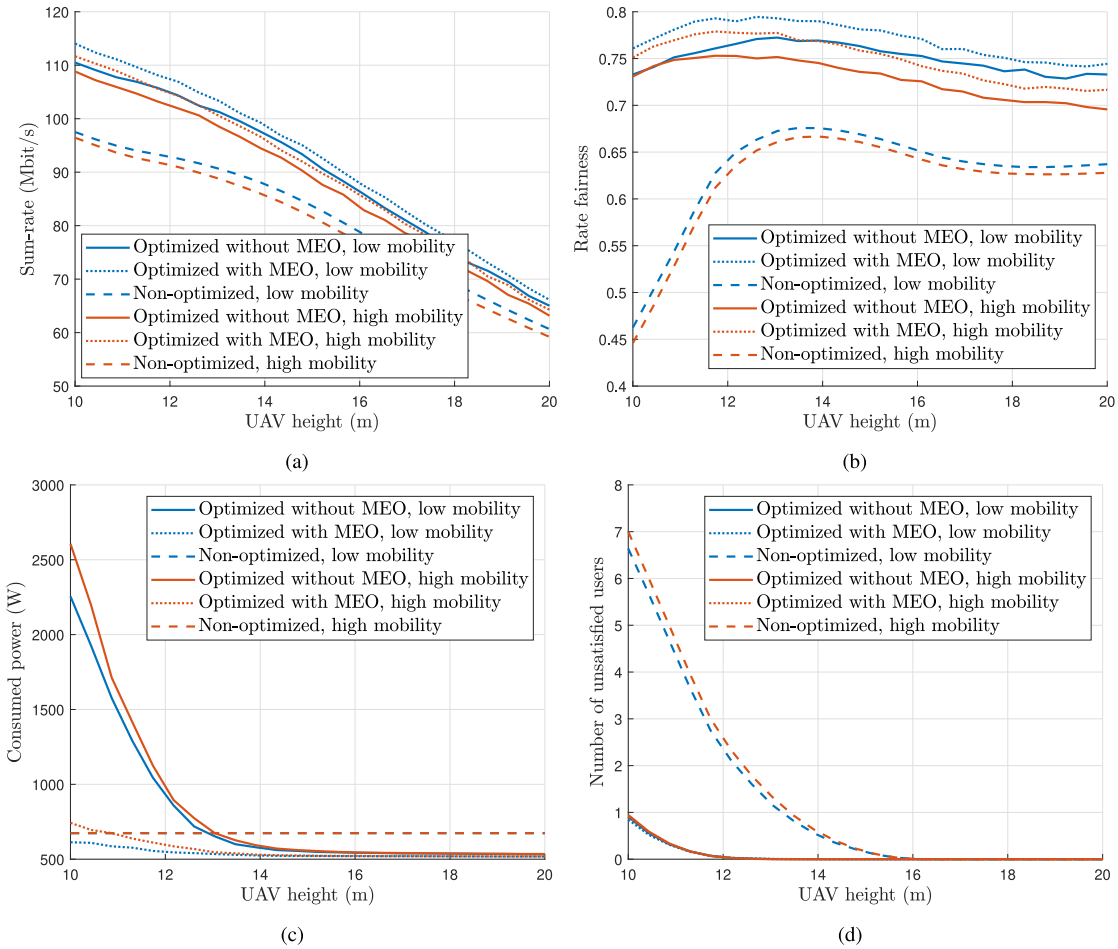

FIGURE 7. Comparison of the effects of non-optimized and optimized UAV locations with and without MEO at different UAVs altitudes for high and low user mobility scenarios. The metrics are (a) the network sum-rate, (b) rate fairness, (c) UAVs power consumption, and (d) number of unsatisfied users.

trajectories are not optimized, their power consumption is independent on their height or on the user mobility, thus retaining a value of 674 W, as shown in Fig. 7(b).

Compared to the baseline case where the UAVs are deployed without optimization, the proposed scheme enhances the system performance as follows:

1) SUM-RATE

Optimizing the UAVs trajectories improves the network sum-rate. At lower altitudes, without MEO, the sum-rate for low and high mobility is 110.5 Mbit/s (a 13.3 % increase) and 108.8 Mbit/s (a 12.8 % increase), respectively, while it is 114.1 Mbit/s (a 17.0 % increase) and 111.7 Mbit/s (a 15.8 % increase) with MEO. The sum-rate gains are more pronounced for low user mobility, as there is a trade-off between the sum-rate and the power consumption of the UAVs. As the user mobility increases, the UAVs need to adjust their positions more frequently and consume more power to maintain the sum-rate. However, since the power consumption of the UAVs is considered in the optimization

problem, the sum-rate performance has to be compromised to avoid excessive power consumption. At higher altitudes, improving the sum-rate is mainly achieved by managing the interference between the UAVs rather than covering new users. Thus, the enhancement in sum-rate is less significant in this case, where the sum-rate for low and high mobility without MEO is 65.0 Mbit/s (a 7.2 % increase) and 63.2 Mbit/s (a 6.7 % increase), respectively, compared to 66.1 Mbit/s (a 9.0 % increase) and 64.2 Mbit/s (an 8.4 % increase) with MEO.

2) RATE FAIRNESS

Optimizing the UAVs trajectories also improves the rate fairness. At lower altitudes, the optimized UAVs trajectories mitigate the blind spots issue, which results in a higher rate fairness of 0.733 (a 58.6 % increase) and 0.731 (a 63.9% increase) for low and high mobility scenarios, respectively, without MEO, compared to 0.760 (a 64.5 % increase) and 0.751 (a 68.1 % increase) with MEO. By optimizing the UAVs locations at higher altitudes, the interference experienced by some users can be minimized. This results in more balanced SINR values among users and leads to a higher rate fairness of 0.733 (a 15.0 % increase) and 0.696 (an 11.0 % increase) for low and high mobility scenarios, respectively, without MEO, compared to 0.744 (a 16.7 % increase) and 0.7167 (a 14.1 % increase) with MEO. The results show that the rate fairness enhancements are more significant at low altitudes, where the problem of blind spots, which cause several users to have no coverage, is more critical than the problem of interference, which causes several users to have low signal quality. In both cases, however, the proposed optimization demonstrates that it can effectively mitigate these challenges and enhance the rate fairness.

3) UAV POWER CONSUMPTION

The optimization of the UAVs trajectories at low altitudes entails high power consumption, as the UAVs have to cope with the blind spots issue by adjusting more frequently to users' movements to meet the data rate constraints. The power consumption in this case may exceed that in the case of non-optimized UAVs trajectories, where the data rate constraints are not considered, resulting in a high number of unsatisfied users, as confirmed by Fig. 7(c). Nonetheless, with the limited computation resources, using the conventional PSO algorithm may not result in converging to a solution that minimizes the number of unsatisfied users with relatively low UAV power consumption. On the other hand, incorporating MEO in the optimization of the UAVs trajectories could lead to significant power savings, as it exploits the temporal correlation between the successive locations of the UAVs and thus enhances the convergence of the algorithm. For instance, at an altitude of 10m, the average power consumption without MEO is 2255.5 W (a 234.6 % increase) and 2606.6 W (a 286.7 % increase) for low and high mobility cases, respectively. By contrast, applying MEO can reduce power consumption to 613.2 W (a 9.0 % decrease) and 742.8 W (a 10 % increase), respectively. Note that the power consumption of the UAVs is proportional to the mobility of the users, as UAVs have to adapt more rapidly to follow the users' movements and improve the sum-rate, rate fairness, and coverage. When the UAVs altitude is relatively high, the coverage constraint is satisfied for all users, and the objective function is mainly influenced by the first three terms that have similar weights. This leads to lower power consumption due to the lower mobility adaptation of the UAVs. Indeed, at an altitude of 20 m, the average power consumption with MEO is 518 W (a 23.1 % decrease) for both low and high mobility, compared to 534 W (a 20.7 % decrease) without MEO.

4) USER COVERAGE

Since the fourth term of the objective function, which aims to minimize the number of unsatisfied users, dominates the other terms, the UAVs tend to prioritize maximizing user coverage over any improvements in sum-rate, rate fairness, and UAVs power consumption. Optimizing the UAV trajectories mitigates the blind spot issue, which reduces the average number of unsatisfied users to 0.95 (an 86.4 % decrease) at low altitudes. Also, it enables providing coverage to all users at a lower height of 14.3 m (a 13.3 % decrease).

The previous results demonstrate the trade-off effect of the UAVs altitude on the system performance metrics. On one hand, deploying the UAVs at low altitudes leads to high sum-rate and high power consumption due to the reduced path loss and the higher need to adapt to user mobility. Conversely, deploying the UAVs at high altitudes leads to low sum-rate and low power consumption due to the increased path loss and the lower need to adapt to user mobility. Nevertheless, both low and high altitudes of the UAVs result in negative impacts on rate fairness due to the limitations on the coverage area and increase in interference, respectively.

D. INTERFERENCE MANAGEMENT

Allocating all the resources of frequency, time, and power to every access point in a wireless network may improve the performance of the users near the center of the cell, but it may also degrade the performance of the users at the cell edge due to inter-cell interference. However, unlike terrestrial systems, UAVs have the advantage of adaptivity, which can be leveraged to avoid or minimize interference from other cells. This can enhance the quality and reliability of the communication links, especially when considering the data rate requirements in the deployment of the UAVs. Moreover, the reliance on LOS communication and the limited FOV of the receivers in VLC networks can be exploited to mitigate inter-cell interference. Therefore, VLC-enabled UAVs can effectively mitigate inter-cell interference that arises when multiple UAVs operate in the same frequency band simultaneously. Here, we compare the approach of managing the

TABLE 2. Impact of interference management methods.

Height	Average data rate (rate fairness)		
	Controlling UAVs deployment	Frequency reuse	Broadcasting
10 m	5.63 (0.73)	1.71 (0.80)	1.22 (0.86)
15 m	4.76 (0.77)	1.64 (0.93)	1.26 (0.95)
20 m	3.27 (0.75)	1.54 (0.94)	1.21 (0.97)
40 m	0.81 (0.85)	0.96 (0.97)	1.00 (0.98)

interference by controlling the UAVs deployment with the following methods:

- Frequency reuse: This method allocates different frequency bands to different UAVs, which would completely eliminate the interference in the cell-edge region [34]. However, this approach has a drawback of reducing the spectral efficiency of the system, as the available resources are not fully utilized for data transmission in each cell. Frequency reuse can effectively mitigate the inter-cell interference effect for cell-edge users and enhance their data rates. In this case, the data rate for the k^{th} user can be computed as:

$$r_k(t) = \frac{BW}{2\,N\,G_k(t)} \log_2\left(1 + \frac{e}{2\pi}\,\frac{\left(\sum_{n=1}^{N} u_{n,k}(t)\,h_{n,k}(t)\,P\right)^2}{N_0\,BW/N}\right). \quad (17)$$

- Broadcasting: In this method, all the UAVs transmit the same signal that carries the data intended for all the users [35]. This method also has the drawback of reducing the overall spectral efficiency of the system. Broadcasting can be very effective when the UAVs are deployed at very high altitudes, where the coverage areas of the UAVs overlap significantly and thus can be exploited to enhance the received signal power. The data rate for the k^{th} user in this method can be computed as:

$$r_k(t) = \frac{BW}{2\,M} \log_2\left(1 + \frac{e}{2\pi}\,\frac{\left(\sum_{n=1}^{N} h_{n,k}(t)\,P\right)^2}{N_0\,BW}\right). \quad (18)$$

The empirical probability density function (pdf) of the users' data rate for different interference mitigation methods and deployment heights is illustrated in Figs. 8(a)-8(d). Table 2 summarizes the average data rate in Mbit/s and the rate fairness for each scenario. It can be observed that there is a significant fraction of users with no coverage when the UAVs are deployed at a height of 10 m, regardless of the interference management method. This is due to the limited coverage area of the UAVs, which can be leveraged to increase the data rate of the users by fully utilizing the available resources with almost no inter-cell interference. This strategy remains effective in delivering high data rates with minor interference when the UAVs height is increased to 15 m, as the UAVs can cope with the impact of inter-cell interference. However, when the UAVs altitude is further increased to 20 m, some unavoidable interference regions emerge, which degrade the performance of the cell-edge users, despite the high average data rates. Hence, frequency reuse and broadcasting become preferable for handling the interference at this height, with the latter resulting in lower data rates, as the overlapping regions between the UAVs are still not large enough to effectively increase the received data rate for most of the users. Operating the UAVs at a very high altitude of 40 m introduces significant inter-cell interference that affects most of the network area, leading to a substantial reduction in the average data rates when the UAVs share the same frequency band. Broadcasting, on the other hand, can be more efficient in this scenario, as it leverages the overlapping regions to enhance the data rate at the receivers. Furthermore, by employing frequency reuse or broadcasting techniques, the system can achieve a higher level of rate fairness among the users. Therefore, the choice of which interference management method to consider depends on the deployment height of the UAVs and the preferable optimization metric. If the UAVs are deployed at relatively low or medium altitudes, or if the sum-rate is the main metric to consider, then relying on the UAVs deployment for interference mitigation would be the suitable option. However, if the UAVs are deployed at high altitudes, or if rate fairness is the main metric to consider, then frequency reuse or broadcasting would be the suitable option.

E. TRADE-OFF ANALYSIS

Different scenarios may require different trade-offs among the network sum-rate, rate fairness, and power consumption. For instance, when power resources are scarce, minimizing power consumption may be prioritized over maximizing the sum-rate or rate fairness. We can adjust such trade-off by tuning the weights η_1, η_2, and η_3. To have a better interpretation of the effect of manipulating the weighting factors, and without loss of generality, we rescale each term in the objective function as follows:

$$\begin{aligned}\max_{\boldsymbol{x}[l],\boldsymbol{y}[l]}\ & \eta_1 \frac{\sum_{k=1}^{K} r_k[l] - \mathbb{E}\left(\min \sum_{k=1}^{K} r_k\right)}{\mathbb{E}\left(\max \sum_{k=1}^{K} r_k\right) - \mathbb{E}\left(\min \sum_{k=1}^{K} r_k\right)} \\ & + \eta_2 \frac{\mathcal{J}(\boldsymbol{r}[l]) - \mathbb{E}(\min \mathcal{J}(\boldsymbol{r}))}{\mathbb{E}(\max \mathcal{J}(\boldsymbol{r}) - \mathbb{E}(\min \mathcal{J}(\boldsymbol{r}))} \\ & - \eta_3 \frac{\sum_{n=1}^{N} q_n[l] - \mathbb{E}\left(\max \sum_{n=1}^{N} q_n\right)}{\mathbb{E}\left(\max \sum_{n=1}^{N} q_n\right) - \mathbb{E}\left(\min \sum_{n=1}^{N} q_n\right)} \\ & - \eta_4\,\overline{N}(R_{\text{th}}) \\ \text{s.t}\ & L/8 \le x_1[l], y_1[l], y_2[l], x_3[l] \le 3L/8, \\ & 5L/8 \le x_2[l], y_3[l], x_4[l], y_4[l] \le 7L/8, \end{aligned} \quad (19)$$

where $\mathbb{E}(\max f(\boldsymbol{x},\boldsymbol{y}))$ and $\mathbb{E}(\min f(\boldsymbol{x},\boldsymbol{y}))$ denote the expected values of the function $f(\boldsymbol{x},\boldsymbol{y})$ when the UAVs trajectory is optimized to achieve the maximum and minimum outcomes, respectively. This transformation ensures a well-scaled objective function, as each term has a comparable magnitude

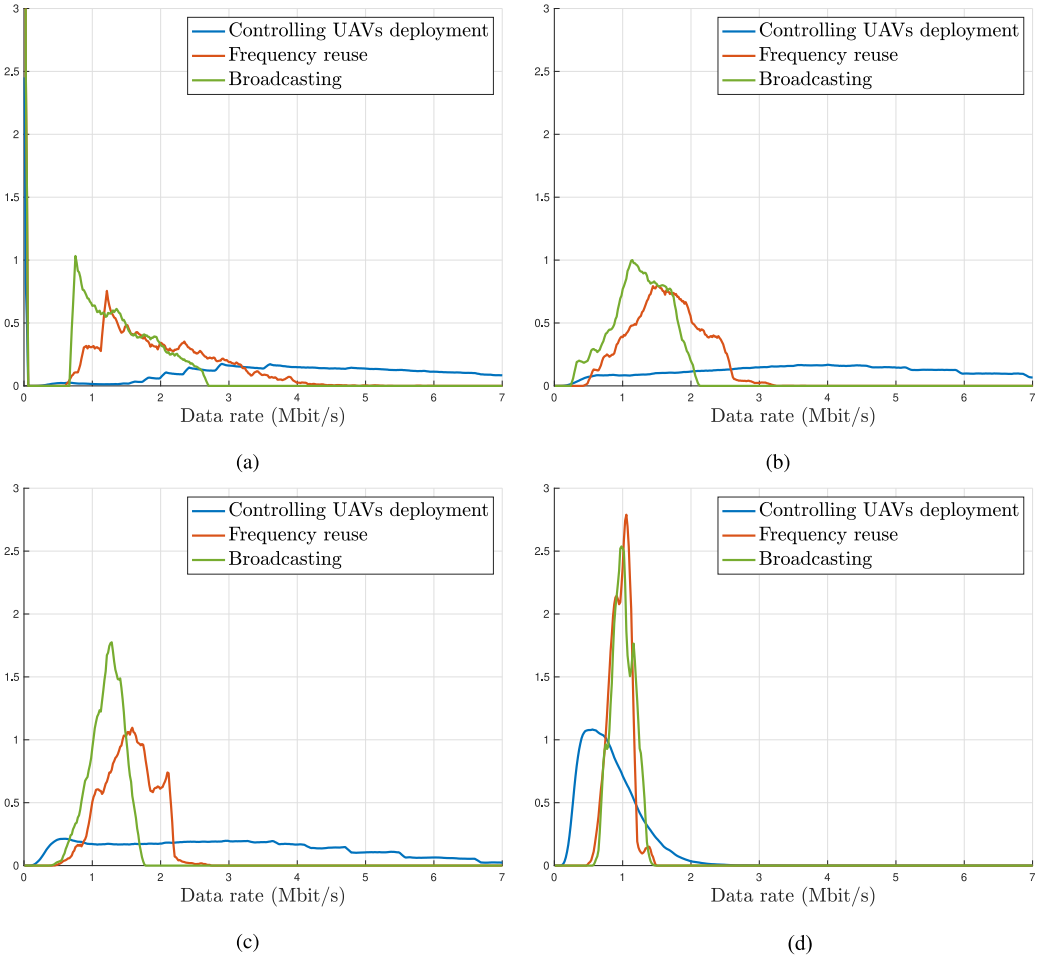

FIGURE 8. Empirical pdf of users' data rate under different interference management methods and different deployment heights of (a) 10 m, (b) 15 m, (c) 20 m, and (d) 40 m.

that is bounded between zero and one. Moreover, if we set the parameters η_1, η_2, and η_3 such that they sum up to one, then the objective function value will also be bounded between zero and one, provided that the data rate constraint is satisfied.

In this study, we consider low user mobility and we use 16 particles and 16 iterations while considering MEO to optimize the locations of the UAVs that operate at an altitude of 16 m. To obtain the values of the constants used in the normalization of the terms, we optimize the UAVs trajectories for two different objectives: maximizing the network sum-rate and maximizing the rate fairness. Both objectives are subject to the data rate constraints. For the first objective, we achieve an average sum-rate of 109.0 Mbit/s, a rate fairness of 0.496, and a consumed power of 1530.0 W. For the second objective, we obtain an average sum-rate of 68.7 Mbit/s, a rate fairness of 0.879, and a consumed power of 2064.3 W. The minimum power consumption for the UAVs equals 504.0 W, which is obtained when they move at a constant velocity of 10.2 m/s, as shown in Fig. 2. Given our interest in optimizing at least one of the considered objectives, it is reasonable to posit that the worst performance of one term is attained when one of the other terms is exclusively considered. Therefore, we normalize the terms in the optimization problem using the following values: 109.0 Mbit/s and 68.7 Mbit/s for the sum-rate, 0.879 and 0.496 for the rate fairness, and 2008.3 W and 504.0 W for the consumed power. Note that without optimizing the UAVs trajectory the average sum-rate, rate fairness, and consumed power are 76.9 Mbit/s, 0.640, and 672.8 W, respectively. This shows that a trade-off should be made between the considered objectives, as optimizing one term individually leads to a worse performance of the others than the case of no optimization. In this study, we use the normalized values to assess the system's performance and report the actual values in parentheses.

Figure 9 shows the trade-off between the normalized sum-rate and normalized rate fairness achieved by optimizing the UAVs locations with different weighting factors. For example, the curve labeled with $\eta_3 = 1/4$ is obtained by fixing η_3 to $1/4$ and varying η_1 and η_2 from 0 to $3/4$ such that $\eta_1 + \eta_2 = 3/4$. We can observe that when the power consumption term is ignored (e.g., $\eta_3 = 0$), the trade-off curve spans from the point $(1, 0)$ to $(0, 1)$, which is consistent with the normalization method used. Nonetheless, the curve is not linear but is concave toward the point $(1, 1)$,

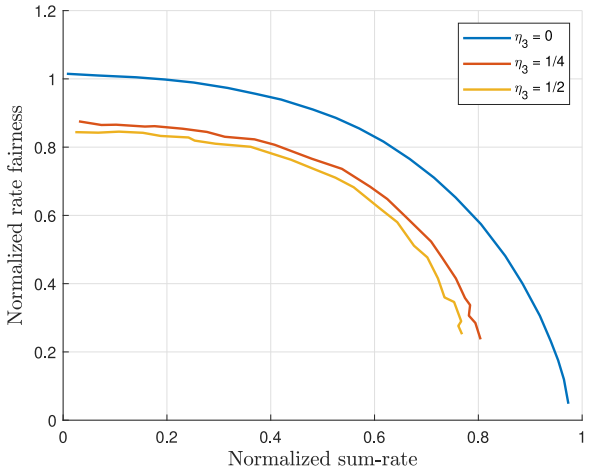

FIGURE 9. The trade-off between normalized sum-rate and normalized rate fairness for different η_3 values. The curves are obtained by optimizing the UAVs locations with different weights η_1 and η_2 that sum up to $1 - \eta_3$.

which implies that by incorporating the network sum-rate and rate fairness in the optimization problem, a relatively high performance in one metric can be achieved without significantly compromising the performance of the other one. For instance, both metrics can simultaneously achieve a performance of 70 % of their normalized dynamic range. Ignoring the power consumption, however, leads to a high average power consumption of 0.404 (1434.0 W).

Incorporating the power consumption term into the optimization problem (e.g., $\eta_3 = 1/4$) reduces the average power consumption to 554.7 W, corresponding to a normalized value of 0.967. However, this significant improvement in the power efficiency was achieved at the expense of lower maximum normalized sum-rate and rate fairness, which decreased from 1 to 0.804 (101.1 Mbit/s) and 0.875 (0.83), respectively. To maintain the same average performance in the sum-rate, the normalized rate fairness would have to decrease by an average value of 0.185 (0.07), which represents the average vertical distance between the curves labeled by $\eta_3 = 0$ and $\eta_3 = 1/4$ in Fig. 9. Alternatively, the average horizontal distance equals 0.235 (9.4 Mbit/s) and represents the average reduction in the normalized sum-rate to maintain the same average performance in the rate fairness. This demonstrates that we can achieve a relatively good performance in sum-rate and rate fairness while substantially reducing the UAV power consumption. The smaller average vertical gap than the horizontal gap can be explained by the higher correlation between optimizing rate fairness and the UAV power consumption, due to the similar distance they induce the UAV to move along compared to the data rate term. This is also why incorporating the power consumption term into the optimization problem leads to an increase in the minimum achievable normalized rate fairness, attained when $\eta_2 = 0$, to a value of 0.236 (0.58). Further increasing η_3 to $1/2$ would decrease the power consumption to 529.0 W, corresponding to a normalized value of 0.983. The maximum normalized sum-rate and rate fairness, in this case, would decrease to 0.768 (9.9 Mbit/s) and 0.84 (0.82), respectively. This indicates that once the power consumption term is included, varying its corresponding weight would not significantly affect the performance of other metrics, as normalized power consumption would already be close to its optimal value.

VI. CONCLUSION

In this work, we presented a novel framework for optimizing the trajectories of VLC-enabled UAVs. Our framework addresses a multi-objective optimization problem that considers the network sum-rate, rate fairness, and power consumption of the UAVs. To solve this problem, we used the PSO algorithm with an enhanced particle initialization. Then, we evaluated the performance of the proposed framework by performing thorough simulation tests, which investigate the parameter selection, algorithm convergence, performance analysis under different deployment heights, and trade-off analysis. The results demonstrated that our framework can adapt the trajectories of the UAVs according to the users' locations and link conditions, and provide a high-quality and energy-efficient communication service for VLC-enabled UAV networks. In general, the proposed optimization can help in mitigating the challenges of blind spots and interference that arise from varying the UAVs altitude, and enhance the reliability and coverage of the network.

REFERENCES

[1] M. Z. Chowdhury, M. Shahjalal, S. Ahmed, and Y. M. Jang, "6G wireless communication systems: Applications, requirements, technologies, challenges, and research directions," *IEEE Open J. Commun. Soc.*, vol. 1, pp. 957–975, 2020.
[2] G. Geraci, D. López-Pérez, M. Benzaghta, and S. Chatzinotas, "Integrating terrestrial and non-terrestrial networks: 3D opportunities and challenges," *IEEE Commun. Mag.*, vol. 61, no. 4, pp. 42–48, Apr. 2023.
[3] Y. Zeng, R. Zhang, and T. J. Lim, "Wireless communications with unmanned aerial vehicles: Opportunities and challenges," *IEEE Commun. Mag.*, vol. 54, no. 5, pp. 36–42, May 2016.
[4] Y. Wang, M. Chen, Z. Yang, T. Luo, and W. Saad, "Deep learning for optimal deployment of UAVs with visible light communications," *IEEE Trans. Wireless Commun.*, vol. 19, no. 11, pp. 7049–7063, Nov. 2020.
[5] H. Ibraiwish, A. Elzanaty, Y. H. Al-Badarneh, and M.-S. Alouini, "EMF-aware cellular networks in RIS-assisted environments," *IEEE Commun. Lett.*, vol. 26, no. 1, pp. 123–127, Jan. 2022.
[6] S. Aboagye, T. M. N. Ngatched, O. A. Dobre, and A. G. Armada, "Energy efficient Subchannel and power allocation in cooperative VLC systems," *IEEE Commun. Lett.*, vol. 25, no. 6, pp. 1935–1939, Jun. 2021.
[7] A. Vavoulas, H. G. Sandalidis, T. A. Tsiftsis, and N. Vaiopoulos, "Coverage aspects of indoor VLC networks," *J. Lightw. Technol.*, vol. 33, no. 23, pp. 4915–4921, Dec. 1, 2015.
[8] Shashikant, P. Garg, and P. K. Sharma, "Interference mitigation technique with coverage improvement in indoor VLC system," *Trans. Emerg. Telecommun. Technol.*, vol. 30, no. 2, p. e3511, 2019.
[9] A. Amantayeva, M. Yerzhanova, and R. C. Kizilirmak, "UAV location optimization for UAV-to-vehicle multiple access channel with visible light communication," in *Proc. Wireless Days (WD)*, 2019, pp. 1–4.
[10] Q.-V. Pham, T. Huynh-The, M. Alazab, J. Zhao, and W.-J. Hwang, "Sum-rate maximization for UAV-assisted visible light communications using NOMA: Swarm intelligence meets machine learning," *IEEE Internet Things J.*, vol. 7, no. 10, pp. 10375–10387, Oct. 2020.

[11] M. W. Eltokhey, M.-A. Khalighi, and Z. Ghassemlooy, "UAV location optimization in MISO ZF pre-coded VLC networks," *IEEE Wireless Commun. Lett.*, vol. 11, no. 1, pp. 28–32, Jan. 2022.
[12] Y. Yang, M. Chen, C. Guo, C. Feng, and W. Saad, "Power efficient visible light communication with unmanned aerial vehicles," *IEEE Commun. Lett.*, vol. 23, no. 7, pp. 1272–1275, Jul. 2019.
[13] Y. Cang et al., "Joint deployment and resource management for VLC-enabled RISs-assisted UAV networks," *IEEE Trans. Wireless Commun.*, vol. 22, no. 2, pp. 746–760, Feb. 2023.
[14] Z. Zhu, Y. Yang, C. Guo, M. Chen, S. Cui, and H. V. Poor, "Power efficient deployment of VLC-enabled UAVs," in *Proc. IEEE 31st Annu. Int. Symp. Pers., Indoor Mobile Radio Commun.*, 2020, pp. 1–6.
[15] M. J. Abdel-Rahman, A. M. AlWaqfi, J. K. Atoum, M. A. Yaseen, and A. B. MacKenzie, "A novel multi-objective sequential resource allocation optimization for UAV-assisted VLC," *IEEE Trans. Veh. Technol.*, vol. 72, no. 5, pp. 6896–6901, May 2023.
[16] M. R. Maleki, M. R. Mili, M. R. Javan, N. Mokari, and E. A. Jorswieck, "Multi-agent reinforcement learning trajectory design and two-stage resource management in CoMP UAV VLC networks," *IEEE Trans. Commun.*, vol. 70, no. 11, pp. 7464–7476, Nov. 2022.
[17] D. N. Anwar, M. Peer, K. Lata, A. Srivastava, and V. A. Bohara, "3-D deployment of VLC enabled UAV networks with energy and user mobility awareness," *IEEE Trans. Green Commun. Netw.*, vol. 6, no. 4, pp. 1972–1989, Dec. 2022.
[18] Y. Zeng, J. Xu, and R. Zhang, "Energy minimization for wireless communication with rotary-wing UAV," *IEEE Trans. Wireless Commun.*, vol. 18, no. 4, pp. 2329–2345, Apr. 2019.
[19] M. S. Demir, S. M. Sait, and M. Uysal, "Unified resource allocation and mobility management technique using particle swarm optimization for VLC networks," *IEEE Photon. J.*, vol. 10, no. 6, pp. 1–9, Dec. 2018.
[20] G. Pau, M. Collotta, V. Maniscalco, and K.-K. R. Choo, "A fuzzy-PSO system for indoor localization based on visible light communications," *Soft Comput.*, vol. 23, pp. 5547–5557, Jul. 2019.
[21] J. M. Kahn and J. R. Barry, "Wireless infrared communications," *Proc. IEEE*, vol. 85, no. 2, pp. 265–298, Feb. 1997.
[22] J.-B. Wang, Q.-S. Hu, J. Wang, M. Chen, and J.-Y. Wang, "Tight bounds on channel capacity for dimmable visible light communications," *J. Lightw. Technol.*, vol. 31, no. 23, pp. 3771–3779, Dec. 1, 2013.
[23] R. K. Jain, D.-M. W. Chiu, and W. R. Hawe, "A quantitative measure of fairness and discrimination," Eastern Res. Lab., Digit. Equip. Corp., Hudson, MA, USA, Tech. Rep. DEC-TR-301, 1984.
[24] R. Ding, F. Gao, and X. S. Shen, "3D UAV trajectory design and frequency band allocation for energy-efficient and fair communication: A deep reinforcement learning approach," *IEEE Trans. Wireless Commun.*, vol. 19, no. 12, pp. 7796–7809, Dec. 2020.
[25] Y. Cai, Z. Wei, S. Hu, C. Liu, D. W. K. Ng, and J. Yuan, "Resource allocation and 3D trajectory design for power-efficient IRS-assisted UAV-NOMA communications," *IEEE Trans. Wireless Commun.*, vol. 21, no. 12, pp. 10315–10334, Dec. 2022.
[26] S. M. Majercik, "GREEN-PSO: Conserving function evaluations in particle swarm optimization," in *Proc. 5th Int. Joint Conf. Comput. Intell.*, 2013, pp. 160–167.
[27] F. Marini and B. Walczak, "Particle swarm optimization (PSO). a tutorial," *Chemometr. Intell. Lab. Syst.*, vol. 149, pp. 153–165, Dec. 2015.
[28] O. Olorunda and A. P. Engelbrecht, "Measuring exploration/exploitation in particle swarms using swarm diversity," in *Proc. IEEE Congr. Evol. Comput. (World Congr. Comput. Intell.)*, 2008, pp. 1128–1134.
[29] J. Robinson and Y. Rahmat-Samii, "Particle swarm optimization in electromagnetics," *IEEE Trans. Antennas Propaga.*, vol. 52, no. 2, pp. 397–407, Feb. 2004.
[30] K. J. Binkley and M. Hagiwara, "Balancing exploitation and exploration in particle swarm optimization: Velocity-based reinitialization," *Inf. Media Technol.*, vol. 3, no. 1, pp. 103–111, 2008.
[31] A. Ratnaweera, S. K. Halgamuge, and H. C. Watson, "Self-organizing hierarchical particle swarm optimizer with time-varying acceleration coefficients," *IEEE Trans. Evol. Comput.*, vol. 8, no. 3, pp. 240–255, Jun. 2004.
[32] F. Bai and A. Helmy, *A Survey of Mobility Models, Wireless Adhoc Netwotk*, vol. 206, Univ. Southern California, Los Angeles, CA, USA, 2004, p. 147.
[33] P. Cazzaniga, M. S. Nobile, and D. Besozzi, "The impact of particles initialization in PSO: Parameter estimation as a case in point," in *Proc. IEEE Conf. Comput. Intell. Bioinf. Comput. Biol. (CIBCB)*, 2015, pp. 1–8.
[34] M. Eltokhey, M. A. Khalighi, and Z. Ghassemlooy, "Multiple access techniques for VLC in large space indoor scenarios: A comparative study," in *Proc. IEEE Int. Conf. Telecommun.*, 2019, pp. 1–6.
[35] Y. Fu, Y. Hong, L.-K. Chen, and C. W. Sung, "Enhanced power allocation for sum rate maximization in OFDM-NOMA VLC systems," *IEEE Photon. Technol. Lett.*, vol. 30, no. 13, pp. 1218–1221, Jul. 1, 2018.

HUSSAM IBRAIWISH (Student Member, IEEE) received the bachelor's degree in electrical engineering from The University of Jordan in 2021, and the master's degree in electrical and computer engineering from the King Abdullah University of Science and Technology in 2023.

MAHMOUD WAFIK ELTOKHEY (Member, IEEE) received the Ph.D. degree from the Institut Fresnel, Ecole Centrale Marseille, France, in 2021. He is a Postdoctoral Fellow with the King Abdullah University of Science and Technology.

MOHAMED-SLIM ALOUINI (Fellow, IEEE) received the Ph.D. degree in electrical engineering from the California Institute of Technology in 1998. He is a Professor with the King Abdullah University of Science and Technology.